International Journal of Engineering Research and Development
e-ISSN: 2278-067X, p-ISSN: 2278-800X, www.ijerd.com
Volume 11, Issue 06 (June 2015), PP.66-74

Numerical Deterministic Method of Including Saturation Effect in the Performance Analysis of a Single-Phase Induction Motor

Peter Michael Enyong
Department of Electrical/Electronic Engineering Technology; Auchi Polytechnic, Auchi, Nigeria.

Abstract:- The effect of magnetic saturation was to be included in the performance analysis of an earlier refurbished single-phase induction motor. The approach was to determine the machine saturation factor by means of a numerical manual computation and to have this factor duly applied on the machine reactances by means of which the saturated version of its reactances were obtained. The latter reactances were then used to realize the required performance parameters of the motor with the non-linear influence of saturation thus included. In this paper, the author details the numerical computations that yielded the saturation factor as K_{sat} =1.18. The saturated machine reactances were then computed giving the value 2.29Ω each for the stator winding reactance and the rotor winding reactance (referred to the stator), and the value 92.79Ω for the magnetizing reactance. Thus, not less than a 15.24% general decrease in the motor reactances was observed. Also, by numerical computations, the motor efficiency, running and starting torques were valued 68.4%, 7.80N-m and 8.14N-m, respectively. Other significant parameters determined under saturation include the input current, no-load current and iron losses whose values were 8.65A, 4.28A and 131.16W, respectively. All these conduced to a 2.92% decrease in the motor efficiency and a 17.1% increase in starting torque, whilst the net output power (in kW) and the motor input power factor (in p.u.) remained virtually unchanged.

Keywords:- Single-phase Motor Parameters, Saturation Effect

I. INTRODUCTION

Apart from skin effect, saturation is another significant non-linear effect which often comes into play in the performance of electrical machines. Indeed, the magnetic circuit in electrical machines gets inevitably saturated in the course of operation. This is usually glaringly observed in the open-circuit characteristic of an electrical machine. The latter comprises the linear "air-gap line" aspect and the non-linear "considerable iron magnetization curve" aspect. For lower values of current input into the stator of an induction motor (meaning lower values of applied voltage) the open-circuit characteristic is a straight line (meaning equal changes in applied voltage give rise to corresponding equal changes in the concomitant input current). However, for higher values of the input current, a departure from a straight-line (or linear) nature is observed, the characteristic now assuming a curvature; indicating the manifestation of saturation according to the books in [1], [2] and the journal in [3]. Despite the advantage of saturation in the realization of higher values of induction motor starting and running torques as reflected in the journal in [4], adequate care is usually taken in the design and construction of the magnetic circuit of an electrical machine to avoid such level of saturation as could impoverish the machine dynamic response according to the book in [5] and the thesis in [6]. Moreover, the presence of saturation in its effect limits the flux in the iron parts of the flux path concerned. Therefore, the usual process in design is to calculate reactances on the assumption of infinite permeability, and then to apply a saturation factor as stated in [5] and the journal in [7].

In arranging this work, the next section (i.e. Section 2) shall deal with the magnetic saturation factor computation from relevant data earlier obtained. In Section 3, the motor saturated reactances shall be determined. The relevant performance parameters with saturation effect shall also be computed. The 4th and last section shall handle discussion, conclusion and recommendation.

II NUMERICAL DETERMINATION OF MAGNETIC SATURATION FACTOR

Determination of rotating machine magnetic saturation factor, K_{sat}, often involves the computation of the magnetomotive force, mmf, for each of the five aspects of the machine magnetic circuit, namely: the air-gap, stator teeth, stator core, rotor teeth and rotor core sections as stipulated in the book in [8]. Consequently, adequate knowledge of the stator and rotor punchings is required. The motor in question as shown in Fig.1 was a 1.5kW, 4-pole, 50Hz, 220V machine. Illustrations of the main parts and punchings are given in Fig.2, 3 and 4. It was dismantled and the stator slots emptied to have all necessary measurements carried out before refurbishment.

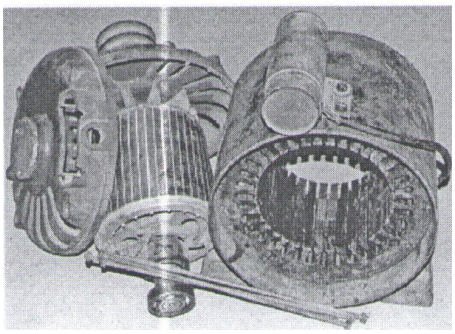

Fig.1: Motor as Dismantled for Measurements and Inspection

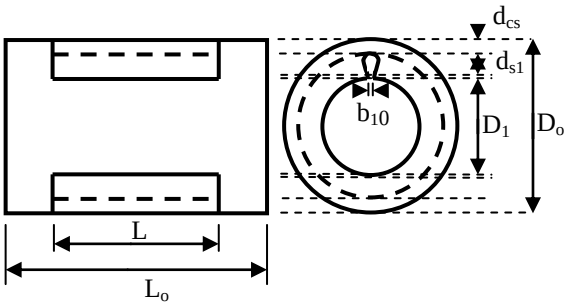

Fig. 2: Overall and Effective Parts and Dimensions of the Stator.

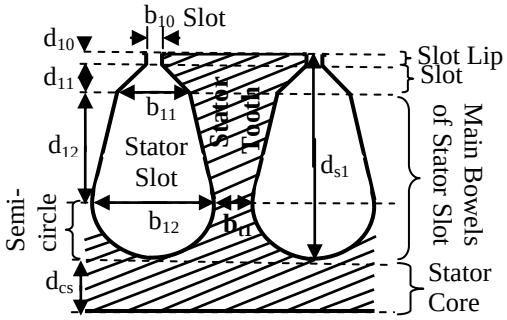

Fig. 3: Round-bottom Stator Slots and Teeth Punching

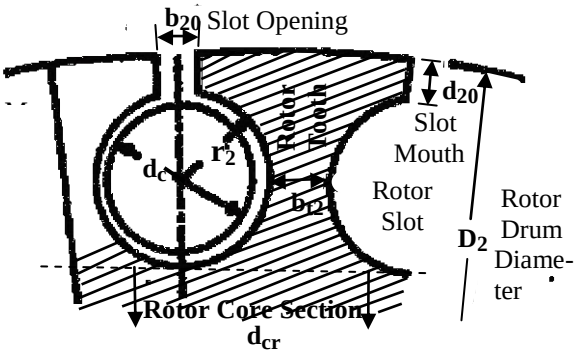

Fig. 4: Rotor Round-Slot and Teeth Punching (d_c *being conductor diameter*)

Details of the measurements taken are: 1) stator bore diameter, D_1 = 13.23cm; 2) stator bore axial length, L = 11.5cm; 3) stator slot opening, b_{10} = 0.3cm; 4) stator slot depth, d_{s1} = 2.26cm; 5) stator tooth width at the narrow end, b_{t1} = 0.55cm; 6) stator core depth, d_{cs}; 7) stator number of slots, S_1 = 36; 8) rotor number of slots, S_2 = 48; and 9) rotor slot opening, b_{20} = 0.08cm. Other significant items made available include a graph for the selection of Carter's Coefficient and a graph of Magnetic Flux Density versus Magnetic Field Intensity (precisely for Lohys core material). The said graphs are given here in Fig.5 and 6, respectively.

From the rated rotor speed, N_r = 1425rpm and considering a slip value, s = 0.05 p.u., the motor synchronous speed, $N_s = N_r/(1 - s) = 1425(1 - 0.05) = 1500$rpm. Thus, the machine number of pole-pairs, $p = (60f)/N_s = (60x50)/1500 = 2$. This parameter is greatly vital in the computations on hand.

A. Computation of the Air-gap Magnetomotive Force, MMF_g

- Air-gap Length, $l_g = 0.013+(0.003D_1/\sqrt{p}) = 0.013+(0.03x13.23/\sqrt{2}) = 0.03$cm.
- Ratio of Stator Slot Opening to Air-gap Length, $b_{10}/l_g = 0.3/0.03 = 10$.
- From the graph of Fig.5, the associated stator Carter's Coefficient for semi-closed slots, $K_{cs} = 0.82$.
- Stator Slot Pitch, $\alpha_s = \pi D_1/S_1 = \pi(13.23/36) = 1.545$cm.
- Stator Gap Coefficient, $K_{gs} = \alpha_s/\{\alpha_s - (b_{10}K_{cs})\} = 1.1545/\{1.1545 - (0.3x0.82)\} = 1.271$.
- Rotor Slot Pitch, $\alpha_r = \pi D_2/S_2$; $D_2 = D_1 - 2l_g = 13.23 - (2x0.03) = 13.17$cm.
  $\therefore \alpha_r = 3.1416x13.17/48 = 0.86$cm.
- Ratio of Rotor Slot Opening to Air-gap Length, $b_{20}/l_g = 0.08/0.03 = 2.67$.

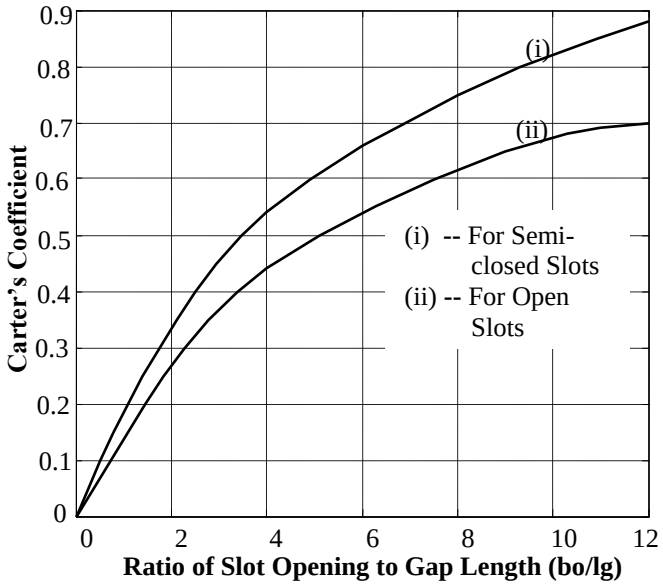

Fig. 5: Carter's Coefficient for Semi-Closed and Open Slots

- From the graph of Fig.5, the associated rotor Carter's Coefficient for semi-closed slots, $K_{cr} = 0.42$.
- Rotor Gap Coefficient, $K_{gr} = \alpha_r/\{\alpha_r - (b_{20}K_{cr})\} = 0.86/\{0.86 - (0.08x0.42)\} = 1.04$.
- Air-gap Coefficient, $K_g = K_{gs}K_{gr} = 1.271x1.04 = 1.322$.
- Air-gap Area, $A_g = \tau L = (\pi D_1/2p)L = \pi D_1 L/2p = 3.1416x13.23x11.5/(2x2) = 119.5cm^2$
- Effective Gap Length, $l'_g = K_g l_g = 1.322x0.03 = 0.04cm$.
- Total Flux per Pole, $\Phi_p = (2/\pi) A_{st} B_{t1}$; $A_{st} = b_{t1}t_p L_i$; $t_p = S_1/(2p)$; $L_i = l_i L$; $l_i = 0.92$ to 0.95.
  where A_{st} – stator teeth area per pole, B_{t1} – stator teeth flux density (1.2 to 1.7T and 1.35T recommended), t_p – stator number of teeth per pole, L_i – effective stator iron length, and l_i – iron stacking factor (0.935 being selected here).
  i.e. $\Phi_p = (2/\pi)b_{t1}S_1/(2p)(0.935L)1.35 = 0.4b_{t1}(S_1/p)L(10^{-4})$ Wb, the multiplying factor of 10^{-4} accounting for conversion of dimensions from cm to m.
  $\therefore \Phi_p = 0.4x0.55x(36/2)x11.5x(10^{-4}) = 0.00455Wb$
- Air-gap Flux Density, $B_g = \Phi_p/\{(2/\pi)A_g\} = 0.00455/\{0.6366x(119.5x10^{-4})\} = 0.598Tesla$.
- ***Air-gap Magnetomotive Force,*** $MMF_g = (1/\mu_0)B_g l'_g = \{1/(4\pi*10^{-7})\}x0.598x(0.04x10^{-2}) =$ ***190AT***.

B. Computation of the Stator Teeth Magnetomotive Force, MMF_{st}

- Magnetic Field Intensity corresponding to the stator teeth flux density, $B_{t1} = 1.35Tesla$ as obtained from the graph of Fig.6 for Lohys punching is $H_{st} = 470AT/m$
- Length of Flux Path in the Stator Teeth, $h_{st} = d_{10} + d_{11} + d_{12}$+bottom semi-circle $= d_{s1} = 2.26cm$
- ***Stator Teeth Magnetomotive Force,*** $MMF_{st} = H_{st}h_{st} = 470x(2.26x10^{-2}) =$ ***10.6AT***

C. Computation of the Stator Core Magnetomotive Force, MMF_{cs}

- Magnetic Flux in the Stator Core Section, $\Phi_{cs} = \Phi_p/2 = 0.00455/2 = 0.002275Wb$
- Sectional Area of Stator Core, $A_{cs} = L_i d_{cs} = 0.935Ld_{cs} = 0.935x11.5x1.9 = 20.43cm^2$
- Magnetic Flux Density in the Stator Core, $B_{cs} = \Phi_{cs}/A_{cs} = 0.002275/(20.43x10^{-4}) = 1.1Tesla$
- Magnetic Field Intensity corresponding to $B_{t1} = 1.11Tesla$ as obtained from the graph of Fig.6 for Lohys punching is $H_{cs} = 230AT/m$
- Length of Flux Path in the Stator Core, $h_{cs} = \{\pi(D_o - d_{cs})/2\}/(2p)$;
  $D_o = D_1 + 2(d_{s1} + d_{cs}) = [\pi(D_1 + 2d_{s1} + d_{cs})/2]/(2p) = [3.1416\{13.23 + (2x2.26) + 1.9\}/2]/(2x2)$
  $= 7.72cm$
- ***Stator Core Magnetomotive Force,*** $MMF_{cs} = H_{cs}h_{cs} = 230x(7.72x10^{-2}) =$ ***17.8AT***

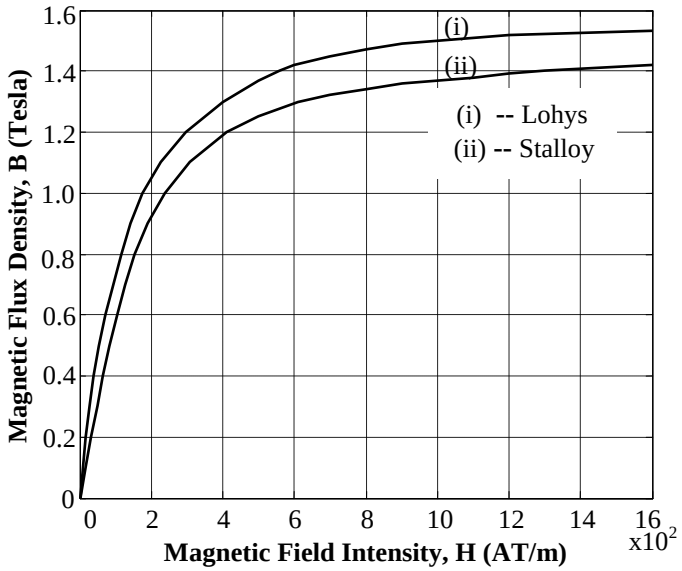

Fig. 6: Magnetization Curves of Two Magnetic Materials

D. Computation of the Rotor Teeth Magnetomotive Force, MMF_{rt}

- Area of all Rotor Teeth per Pole, $A_{rt} = L_i b_{t2}(S_2/2p)$; b_{t2} = (0.9 to 0.95)$(S_1/S_2)b_{t1}$, and with a typical factor of 0.95 being adopted, b_{t2} = 0.95)(36/48)(0.55) = 0.3919cm

: . $A_{rt} = 0.935Lb_{t2}(S_2/2p) = 0.935x11.5x0.3919x48/(2x2) = 50.57cm^2$

- Magnetic Flux Density in the Rotor Teeth, $B_{t2} = \Phi_p/\{(2/\pi)A_{rt}\} = 0.00455/\{(2/\pi)(50.57x10^{-4})\}$ = 1.4Tesla
- Magnetic Field Intensity corresponding to B_{t2} = 1.4Tesla as obtained from the graph of Fig.6 for Lohys punching is H_{rt} = 560AT/m
- Length of Flux Path in the Rotor Teeth, $h_{rt} = 2r_2+d_{20}$; d_{20} to be assumed equal to b_{20} (= 0.07 to 0.08cm where not given or measured, according to [14]). Here by measurement b_{20} = 0.08cm = d_{20}. The radius of rotor slot circle, $r_2 = [\pi\{D_2 - 2d_{20}\} - S_2b_{t2}]/\{2(S_2 + \pi)\}$
  = [3.1416{13.17 – (2x0.08)} – (48x0.3919)]/{2x(48+3.1416)} = 0.2157cm
  : . h_{rt} = (2x0.2157) + 0.08 = 0.5114cm
- ***Rotor Teeth Magnetomotive Force,*** $MMF_{rt} = H_{rt}h_{rt} = 560x(0.5114x10^{-2})$ = ***2.9AT***

E. Computation of the Rotor Core Magnetomotive Force, MMF_{cs}

- Magnetic Flux in the Rotor Core Section, $\Phi_{cr} = \Phi_p/2 = 0.00455/2 = 0.002275Wb$
- Sectional Area of Rotor Core, $A_{cr} = L_i d_{cr}$; d_{cr} being safely assumed as $0.95d_{cs}$(=1.805cm) i.e. $A_{cr} = (0.935L)(0.95d_{cs}) = (0.935x11.5)x1.805 = 19.4cm^2$
- Magnetic Flux Density in the Rotor Core, $B_{cr} = \Phi_{cr}/A_{cr} = 0.002275/(19.4x10^{-4}) = 1.17$Tesla
- Magnetic Field Intensity corresponding to B_{cr} = 1.17Tesla as obtained from the graph of Fig.6 for Lohys punching is H_{cs} = 280AT/m
- Length of Flux Path in the Rotor Core, $h_{cr} = [\pi\{2r_2+d_{20}+ d_{cr}\}/2]/(2p)$;
  = [3.1416{(2x0.2157)+0.08+1.805}/2]/(2x2) = 0.9097cm
- ***Rotor Core Magnetomotive Force,*** $MMF_{cs} = H_{cs}h_{cs} = 280x(0.9097x10^{-2})$ = ***2.5AT***

F. Computation of the Magnetic Saturation Factors

- Total Motor Magnetomotive Force, MMF_{tot} = 190 + 10.6 + 17.8 + 2.9 + 2.5 = 224
- Magnetic Saturation Factor, $K_{sat} = MMF_{tot}/MMF_g = 224/190 = 1.18$
- The Ratio of All Iron Magnetomotive Force (MMF_{ir}) to Gap Magnetomotive Force is given as Specific Magnetic Saturation Factor, K'_{sat} = (10.6 + 17.8 + 2.9 + 2.5)/190 = 0.18

II. SATURATED EQUIVALENT CIRCUIT & PERFORMANCE PARAMETERS

A. Complete Equivalent Circuit of the Single-Phase Induction Motor

The performance details of a given motor are often obtained by means of the equivalent circuit parameters of the machine, which are themselves obtainable from the relevant complete equivalent circuit of the motor. An equivalent circuit of a machine has been defined as *a system of static elements in which the currents*

and voltages satisfy the same equations as the machine according to the book in[9]. The complete equivalent circuit of a single-phase motor is as shown in Fig.7 and arises from the fact that current in a single-phase winding produces a pulsating magnetic field, not a rotating one which is applicable to the 3-phase motors.

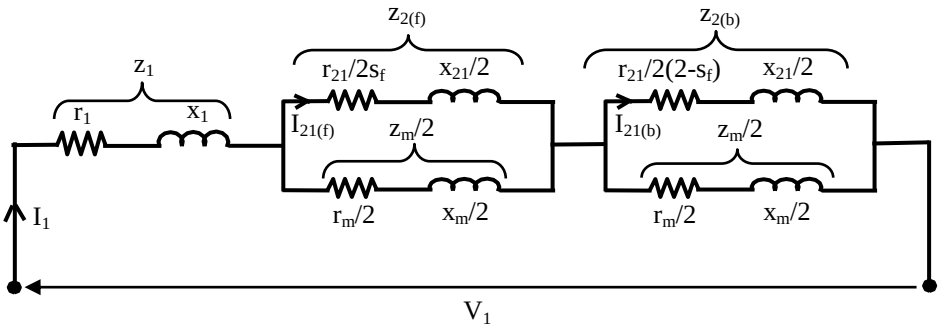

Fig. 7: Complete Equivalent Circuit of a Single-Phase Induction Motor

Thus, the performance analysis of a single-phase motor can only be placed on the same basis as the 3-phase version if its pulsating magnetomotiveforce (mmf) is represented by two fields of constant amplitude rotating in opposite directions as found in the books in [10], [11].

B. Determination of the Saturated Motor Parameters:

1) The Equivalent Circuit Resistances and Saturated Reactances: As of a standard stipulation in [12], the equivalent circuit parameters are often determined by means of three tests, namely: stator winding d.c. resistance test, open-circuit test and short-circuit test. The unsaturated reactances and the temperature-corrected resistances as earlier obtained from these tests have the values: $r'_1 = 2.526\Omega$ (corrected stator winding resistance), $r'_{21} = 2.584\Omega$ (corrected rotor winding resistance referred to stator), $r'_m = 14.34\Omega$ (corrected core-loss resistance), $x_1 = x_{21} = 2.702\Omega$ (unsaturated stator and rotor winding reactances, respectively) and $x_m = 109.49\Omega$ (unsaturated magnetizing reactance) as found in the thesis in [13]. The resistances were obtained at 35^oC and needed to be corrected to their values at 75^oC following the standard provided in [14].

It is to be noted that, the saturation factor, K_{sat}, is as well defined in terms of equivalent circuit reactances as the ratio of $x_{(unsaturated)}$ to $x_{(saturated)}$; where the saturated equivalent circuit reactance, $x_{(saturated)}$, is that obtained from a full-voltage short-circuit test at 75^oC according to [14]. Hence, the saturated version of the equivalent circuit reactances were now realized as $x'_1 = x'_{21} = 2.702/1.18 = 2.29\Omega$ (for the stator and rotor windings, respectively) and $x'_m = 109.49/1.18 = 92.79\Omega$ (for the magnetized core or iron).

2) The Relevant Motor Performance Parameters with Saturation Effect: These were obtained from the solution of the complete equivalent circuit using the saturated reactances and corrected resistances under the following conditions: full-load (with slip, $s_f = 0.05$), open-circuit (with slip, $s_f = 0$) and short-circuit (with slip, $s_f = 1$).

Under Full-Load Condition –

$Z_1 = 2.5265 + j2.29$ (stator impedance)

$Z_{2(f)} = 25.84 + j1.145 = 25.8654\angle(2.54^o)$ (forward rotor impedance)

$Z_m/2 = 7.17 + j46.4 = 46.9507\angle(81.22^o)$ (i.e. ½ core magnetizing impedance)

$Z_{2(b)} = 0.6626 + j1.145 = 1.3229\angle(59.94^o$ (backward rotor impedance)

Let $Z_{2(fp)}$ and $Z_{2(bp)}$ be the effective impedances of the forward and backward paralleled circuits, respectively. Thus,

$Z_{2(fp)} = Z_{2(f)}*(Z_m/2)/\{Z_{2(f)} + (Z_m/2)\} = 20.981\angle(28.53^o) = 18.4332 + j10.0209$

$Z_{2(bp)} = Z_{2(b)}*(Z_m/2)/\{Z_{2(b)} + (Z_m/2)\} = 1.289\angle(60.51^o) = 0.6345 + j1.122$

Motor input impedance is obtained as

$Z_{in} = Z_1 + Z_{2(fp)} + Z_{2(bp)} = 21.3131 + j13.3832 = 25.43\angle(31.88^o)$

The full-load input current is realized as

$\mathbf{I_{in}} = V_1/Z_{in} = \{220\angle(0^o)\}/\{25.43\angle(31.88^o)\} = \mathbf{8.6512\angle(-31.88^o)}$

Input power factor on full load is

$\mathbf{\cos\phi_{in}} = \cos 31.88^o = \mathbf{0.849\ p.u.}$(lagging)

Forward and backward rotor currents are, respectively

$I_{21(f)} = I_{in}*[(Z_m/2)/\{Z_{2(f)} + (Z_m/2)\}] = 7.0175\angle(-5.89^o)$

$I_{21(b)} = I_{in}*[(Z_m/2)/\{Z_{2(b)} + (Z_m/2)\}] = 8.4294\angle(-31.31^o)$

For a 4-pole 50Hz motor, the synchronous speed is

$n_s = f/p = 50/2 = 25$rps (where 'p' is number of pole-pairs)

Hence, the forward and backward mechanical torque values are, respectively

$T_{m(f)} = I^2_{21(f)}*[(r'_{21}/2s_f)/(2\pi n_s)] = 7.0175^2[\{2.584/(2*0.05)\}/(2\pi*25)] = 8.101$N-m

$T_{m(b)} = I^2_{21(b)}*[(r'_{21}/\{2(2-s_f)\})/(2\pi n_s)] = 8.4294^2[\{2.584/(2(2-0.05))\}/(2\pi*25)]$

$= 0.2997$N-m

Net forward or approximate nominal mechanical torque

$\mathbf{T_{mn}} = T_{m(f)} - T_{m(b)} = 8.101 - 0.2997 =$ **7.8013N-m**

Nominal mechanical output power

$\mathbf{P_{mn}} = 2\pi n_r T_{mn} = 2\pi n_s(1-s_f)T_{mn} = 2\pi*25(1-0.05)*7.801 =$ **1164W**

Total stator and rotor copper losses

$P_{co(s)} = I^2_{in}*r'_1 = 8.6512^2(2.5265) = 189.09$W (total stator copper loss)

$P_{co(r)} = I^2_{in}*r'_{21} = 8.6512^2(2.584) = 193.39$W (total rotor copper loss)

Under No-Load or Open-Circuit Condition –

$Z_{oc} = Z_1 + (Z_m/2) + Z_{2(b)}$ (open-circuit input impedance)

$= (2.5265 + 7.17 + 0.6626) + j(2.29 + 46.9507 + 1.145)$

$= 10.3591 + j50.3857 = 51.4396\angle(78.38^o)$

Therefore, the motor input current can be obtained as

$\mathbf{I_{oc}} = V_1/Z_{oc} = \{220\angle(0^o)\}/\{51.4396\angle(78.38^o)\} =$ **4.277∠(-78.38°)A**

$\cos\phi_{oc} = \cos 78.38^o = 0.2014$ (open-circuit power factor)

Total core or iron losses, friction & windage losses and stray or additional losses

$\mathbf{P_{ir}} = I^2_{oc}*(r'_m/2) = 4.277^2(14.34/2) =$ **131.1589W** (core or iron losses)

Friction & windage losses (P_{FW}) ranges from 0.01 to $0.02P_{mn}$ as in the journal in [15] and 0.015 factor was used. Stray or additional losses (P_{add}) is often taken as 0.005Pmn as in [13].

: . $P_{FW} = 0.015*1164 = 17.46$W and $P_{add} = 0.005*1164 = 5.82$W.

Motor total losses and efficiency now stand out, respectively, as

$P_{loss} = P_{co(s)} + P_{co(r)} + P_{ir} + P_{FW} + P_{add} = 536.92$W

$\mathbf{Eff} = P_{mn}/(P_{mn} + P_{loss})*100 = 1164/(1164 + 536.92)*100 =$ **68.4%**

Under Short-Circuit Condition –

The effective impedances involved under this condition are Z_1, $Z_{2(f)}$ and $Z_{2(b)}$ all in series, where essentially $Z_{2(f)}$ and $Z_{2(b)}$ are equal (as ***s = 1*** in this case). Therefore, the short-circuit impedance is

$Z_{sc} = Z_1 + 2Z_{2(f)} = [2.5265 + 2(1.292)] + j[2.29 + 2(1.145)]$

$= 5.1105 + j4.58 = 6.8625\angle(41.87^o)$

Short-circuit current on full voltage and the power factor

$\mathbf{I_{sc}} = V_1/Z_{sc} = \{220\angle(0^o)\}/\{6.8625\angle(41.87^o)\} =$ **32.06∠(-41.87°)A**

Starting Torque, T_{ms}, on full voltage (reflecting saturation condition) is given by

$\mathbf{T_{ms}} = T_{mn}*[I_{sc}/I_{21(f)}]^2*s$

$=$ **7.801*[32.06/7.0175]²*0.05 = 8.1411N-m**

III. DISCUSSION, CONCLUSION AND RECOMMENDATION

A. Discussion

The machine saturation factor, $K_{sat} = 1.18$ was good, showing moderate saturation condition. According to [10] K_{sat} usually lies between 1.1 and 1.25 in typical machines. Fig.8 shows the graph of average flux density factor, α_i, as a function of K'_{sat}. And as evidenced from the said graph, the factor $\alpha_i = 0.70$ approximately for $K'_{sat} = 0.18$, depicting moderate tooth saturation according to [11]. Again, since the Average Flux Density or Specific Magnetic Loading, $B_{av} = \alpha_i B_g = 0.70x0.598 = 0.42$Tesla, the question of moderate saturation is further clarified, being that B_{av} ranges in practice from 0.3 to 0.6Tesla as found in the journal in [16].

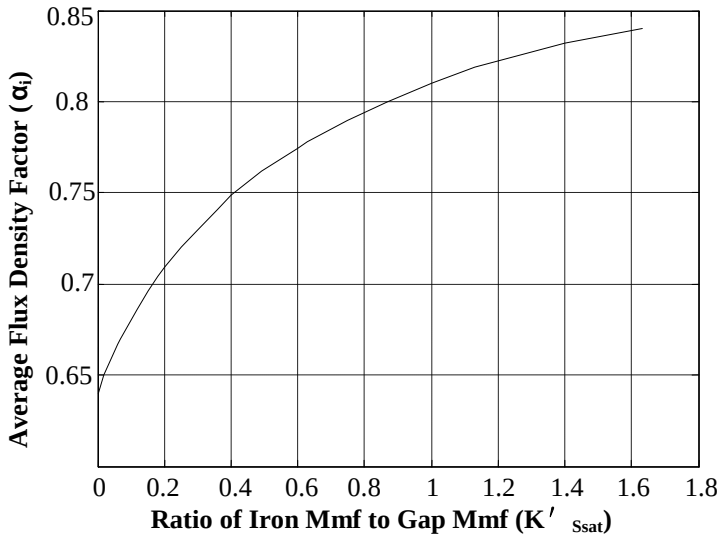

Fig. 8: Average Flux Density Factor (α_i) as a Function of K'_{sat}

For the purpose of comparison, the result of a MATLAB-based computer-aided technique evolved by the author in [13] for squirrel-cage induction motor design and performance calculations (as applicable to the motor in question) is here presented as affecting the unsaturated version of the motor parameters.

CADTECH DETAILS OF THE MOTOR PERFORMANCE PARAMETERS
AT 75 DEG. CENT. WITHOUT MAGNETIC SATURATION EFFECT

1] THE MACHINE RESISTANCES AND REACTANCES:
Stator_Corrected_Resistance_in_Ohms =
2.5265
Rotor_Corrected_Resistance_in_Ohms =
2.5840
Core_Loss_Corrected_Resistance_in_Ohms =
14.3395
Stator_Unsaturated_Reactance_in_Ohms =
2.7017
Rotor_Unsaturated_Reactance_in_Ohms =
2.7017
Core_Unsaturated_Magnetising_Reactance_in_Ohms =
109.4925
2] THE MOTOR CIRCUIT CURRENTS:
Rated_Motor_Input_Current_in_Amps =
8.2557
Exciting_Current_on_Full_Voltage_in_Amps =
3.6625
ShortCircuit_Current_on_Full_Voltage_in_Amps =
29.5803
3] THE MOTOR POWER LOSSES:
Stator_Copper_Loss_in_Watts =
172.1995
Rotor_Copper_Loss_in_Watts =
176.1131
Total_Copper_Losses_in_Watts =
348.3126
Total_Iron_Losses_in_Watts =
96.1767
Friction_and_Windage_Losses_in_Watts =

```
            17.4475
Stray_or_Additional_Load_Losses_in_Watts =
             5.8158
4] THE MOTOR POWER FACTORS:
Rated_Motor_Input_Power_Factor_in_PerUnit =
             0.8589
No_Load_Power_Factor_in_PerUnit =
             0.2044
Short_Circuit_Power_Factor_in_PerUnit =
             0.6871
5] THE ACTIVE POWER QUANTITIES:
Gross_Mechanical_Output_Power_in_Watts =
          1.2768e+003
Net_Mechanical_Output_Power_in_Watts =
          1.1632e+003
Maximum_Mechanical_Output_Power_in_Watts =
          1.6898e+003
6] THE DEVELOPED TORQUE DETAILS:
Gross_Mechanical_Output_Torque_in_Nm =
             8.5561
Forward_Mechanical_Torque_Component_in_Nm =
             8.0679
Backward_Mechanical_Torque_Component_in_Nm =
             0.2732
Net_Forward_Mechanical_Output_Torque_in_Nm =
            7.7947
Maximum_Mechanical_Output_Torque_in_Nm =
            14.3436
Mechanical_Starting_Torque_in_Nm =
             6.9531
7] THE MOTOR EFFICIENCY:
Machine_Percentage_Efficiency =
            71.3197
8] THE MOTOR NOMINAL SLIP VALUE SELECTED:
Machine_Full_Load_Slip_in_PerUnit =
             0.0500
DONE
>>
```

It will be observed that the motor stator and rotor reactances were reduced by 15.24% each; the magnetizing reactance was reduced by 15.25%. Generally, the motor reactances were reduced by not less than 15.24% owing to saturation. The machine efficiency was also reduced in value from what obtains without saturation by 2.92%; whereas, the no-load current, short-circuit current, iron losses and starting torque became increased by the values 16.78%, 8.38%, 36.37% and 17.1%, respectively, under saturation condition.

IV. CONCLUSION

From the analysis in this paper, it is conclusive that saturation has the effect of decreasing a motor magnetizing reactance considerably, bringing about an increase in the no-load current and a consequent increase in core losses; hence, causing a drop in the machine efficiency; the gain as to improvement of starting torque notwithstanding.

V. RECOMMENDATION

By virtue of all the above, it is recommendable that magnetic saturation should be kept as low as good motor starting properties would allow. This can only be achieved right at the machine design stage by way of proper selection of the magnetic core material, proper stator and rotor slot/tooth punching, proper air-gap radial length selection, proper selection/arrangement/connection of windings, amongst other requirements.

REFERENCES

[1] Jackson K. G. (1973): Dictionary of Electrical Engineering; London; Newnes-Butterworths; p.246.

[2] Gupta J. B.(2005): Theory and Performance of Electrical Machines; 14th Ed.; Nai Sarak, Delhi; S. K. Kataria & Sons; p.385.

[3] Ouadu H. et al (2011): Accounting for Magnetic Saturation in Induction Machines Modeling; International Journal of Modeling and Control; Vol. 14, No. 1, 2; pp.27-36.

[4] Kasmieh T. et al (2000): Modeling and Experimental Characterization of Saturation Effect of an Induction Machine; The European Physical Journal (Applied Physics); EDP Sciences; Vol. 10; pp123-130.

[5] Say M. G. (1976): Alternating Current Machines, 4th Ed., London, Pitman Publishing Limited; p.264.

[6] Mikaela Ranta (2013): Dynamic Induction Machine Models including Magnetic Saturation and Iron Losses; Doctoral Dissertation 171/2013; Finland; Aalto University Publication Series; p.21-39.

[7] Su-Yeon C. et al (2013): Characteristics Analysis of Single-phase Induction Motor via Equipment Circuit Method and Considering Saturation Factor; Journal of Electrical Engineering Technology; Vol. 8; pp. 742-747.

[8] Mittle V. N. & Mittal A. (1996): Design of Electrical Machines, 4th Ed., Nai Sarak, Delhi, Standard Publishers Distributors; p.29-54; 412-465.

[9] Adkins B. & Harley R. G. (1975): The General Theory of Alternating Current Machines, Application to Practical Problems; London; Chapman & Hall Ltd. p.47.

[10] Fitzgerald A. E., Kingsley C. Jr. & Umans S. D. (2003): Electric Machinery, 6th Ed., New Delhi, Tata McGraw-Hill Book Publishing Company Limited; p. 183-191, 231.

[11] Pyrhonen J., Jokinen T. & Hraboveova V. (2008): Design of Rotating Electrical Machines; Chichester, West Sussex, P0198SQ, UK; John Wiley & Sons Ltd.; p.303-305; 313-370.

[12] IEEE Standard 112(1996): Standard Test Procedure for Poly-phase Induction Motors and Generators; IEEE Publication.

[13] Enyong P. M. (2014): Computer Software Application in the Redesign and Refurbishment of Squirrel-Cage Induction Motors; PhD research work, presented at a PG School Defense Forum, University of Benin, Benin-City, Nigeria.

[14] Liwschitz-Garik M. and Whipple C. C. (19--): Alternating Current Machines, 2nd Ed., Princeton, New Jersey, D. Van Nostrand Co. Inc.; p.244; 162-181.

[15] Ayasun S. & Nwankpa C. O. (2005): Induction Motor Tests using MATLAB/Simulink and Their Integration into Undergraduate Electric Machinery Courses; IEEE Trans. on Education; Vol. 48, No. 1; pp. 37-46.

[16] Enyong P. M. & Ike S. A. (2014): Development and Application of Machine Design Equations for Computer-Aided Design of Single-Phase Induction Motor; Journal of Mathematics and Technology; Vol. 5, No. 2; pp. 43-54.